

Thermonuclearly-Driven Cellular Structure of Detonation on the Surface of a White Dwarf

Kazuya Iwata^a, Keiichi Maeda^b

^a Department of Mechanical Engineering and Science, Kyoto University

Nishikyo-ku, Kyoto, Japan

^b Department of Astronomy, Kyoto University

Sakyo-ku, Kyoto, Japan

1 Introduction

Astrophysical detonation, which is driven by thermonuclear reactions, is known to drive energetic astronomical phenomena. One major example is Type Ia supernovae (SNe Ia). In SNe Ia, a white dwarf (WD), which is a final state of a low-to-medium mass star, explodes as a result of a thermonuclear runaway, initiating at the center of its core consisting of carbon and oxygen, off the center in its core, or at the interface of the core and the envelope of helium-rich materials. Direct initiation of detonation or Deflagration-to-Detonation Transition (DDT) depends on the system considered: if the WD reaches near-Chandrasekhar mass (~ 1.4 times the solar mass), DDT is favorable for the consistency with the observations, while the direct initiation is allowable for sub-Chandrasekhar mass WDs. Although the cellular structure is expected to exist in these detonations as is so in terrestrial chemical detonation, understanding of this aspect is still lacking to date. Gamezo et al. [1], and Timmes et al. [2] once investigated the cellular structure of astrophysical detonation expected in the carbon/oxygen WD core where the density is the orders of 10^6 - 10^7 g/cm³. They conducted two-dimensional simulations applying the grid sizes of 10^{-2} - 10^2 cm including a nuclear reaction network of 13 isotopes [3], in which the cellular structures were observed with cell widths of 1 - 10^4 cm. A delay in the reaction was observed compared to the one-dimensional Zel'dovich-von Neumann Doring (ZND) theory [2]. The characteristic point of astrophysical detonation is that multiple cell widths can be defined depending on what stage of the thermonuclear reaction process is considered: namely, carbon to oxygen, oxygen to silicon, or silicon to iron. The cell widths of the latter reactions may be larger than the size of the core or the whole WD, which could end up producing intermediate-mass elements (IMEs) including silicon while hindering the production of iron-group elements (IGEs). This difference in the cell width could provide different outcomes in nucleosynthesis depending on the WD considered, which may be important to constrain the progenitor system for SNe Ia.

Thus, studies on the cellular physics of astrophysical detonation could benefit the understanding of the major progenitor of SNe Ia, on which there is still no consensus yet to date. One recent concern is sub-Chandrasekhar mass explosion, which is known as the double-detonation scenario, in which detonation initiated in the helium-rich envelope induces the secondary detonation at the WD core [4-6]. Detonation in the helium-rich envelope in this scenario has not been studied much from the perspective of cellular physics. The existence of the cellular structure was partly indicated in the works by Moore et al. [7], but

quantitative analysis of the cellular structure of the helium-rich detonation has never been done yet so far. In the present study, the authors investigate the detailed structure of helium-rich detonation in the WD envelope by conducting two-dimensional simulations and quantifying the cell widths depending on the density and the composition of the envelope. ZND theoretical analysis is also conveyed to provide the scales of the thermonuclear reaction. These studies would benefit the understanding of the dynamics of the primary explosion in SNe Ia and constraining the systems available for normal type SNe Ia.

2 ZND Theoretical Aspects of Helium-rich Detonation

The one-dimensional structure of the helium-rich detonation is first addressed via ZND theory. A reaction network of 13 isotopes [3] is applied to provide the Hugoniot curve. Bader-Deuflhard method [8], which is an iterative implicit method suitable for the time integration of a stiff reaction system, is used to advance the reaction in time. The intersection of the Hugoniot curve thereby calculated and the Rayleigh line, the slope of which is provided by Chapman-Jouguet (C-J) theory [9, 10], is acquired with the bisection method at each longitudinal location.

Density is varied $\rho = 10^5$ - 10^6 g/cm³, and helium mass fraction is varied between 0.0 – 1.0 with the rest being an equal amount of carbon and oxygen. Fig. 2 illustrates some of the obtained 1D profiles for variable compositions with a constant density of $\rho = 10^6$ g/cm³. In each figure, the abscissa is the post-shock distance in a logarithmic form, and 1D profiles of temperature, density, energy generation rate, and mass fractions of the isotopes are shown. The multi-stage nature of astrophysical detonation is represented well here: with carbon included (Fig. 2(a)-(c)), carbon to oxygen, oxygen to silicon, and silicon to nickel via the α -capture (capture of ⁴He) reaction. Without helium in the initial mixture (Fig. 2(a)), helium must be produced in the first place by heavy-ion reactions. Without carbon and oxygen (Fig. 2(d)), the production of carbon proceeds via a triple- α reaction. Production of oxygen and silicon is soon followed by the final stage of nickel production. It is also noted in each figure that the distance to the final equilibrium state is extremely long, over the order of 10^8 cm, which is comparable to the size of WD. Thus, C-J detonation is almost always not likely to be realized. However, because discussion on this issue makes a comparative study much more complicated, we start with a basic consideration of the C-J properties of each detonation.

What is common to every case including those not shown in Fig. 2 is that the maximum energy generation rate is almost coincident with the maximum production or concentration of silicon. The distance to this maximum energy generation strongly depends on the mass fraction of helium: the existence of helium boosts up the reaction of ¹²C+⁴He \rightarrow ¹⁶O, resulting in a shorter distance to the following reaction stages. However, in pure helium (Fig. 2(d)), this reaction stage is delayed for the absence of carbon in the initial mixture. With helium in the initial mixture, helium remains $\sim 10^{-4}$ - 10^{-2} in the mass fraction at the equilibrium state.

In the simulations of terrestrial detonation, a criterion of the resolution is based on the half-reaction length of the fuel. Gamezo et al. [1] determined a resolution based on the half-reaction length of carbon since they considered only the detonation of carbon and oxygen at the WD core. This is clearly not appropriate for pure-helium detonation, but in the following 2D study, the range of helium mass fraction is 0.0-0.8 omitting pure helium. Hence, the same criterion is used for comparison with these previous studies, placing about 20 grids in the carbon half-reaction length.

3 Two-dimensional simulation

A simple two-dimensional domain is used to define a detonation-fixed non-inertial coordinate. The inlet velocity is controlled to balance the propagation velocity of the detonation, by canceling their gap by adding inertial force to decelerate or accelerate the whole system. Grid size is uniform throughout the domain and is arranged in each computational case so that about 20 grids are contained in the induction region, which is defined in this study between the shock and the location at which carbon is half-consumed. The total grid number is fixed to be 2000 x 1200. Lateral boundaries are treated as periodic.

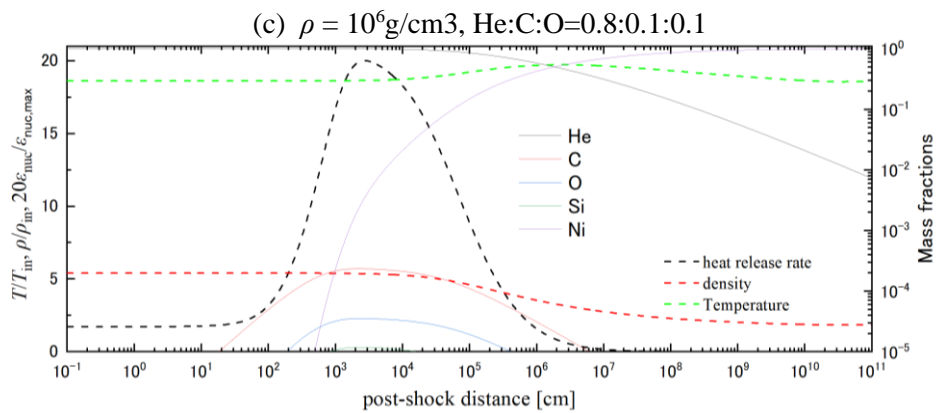
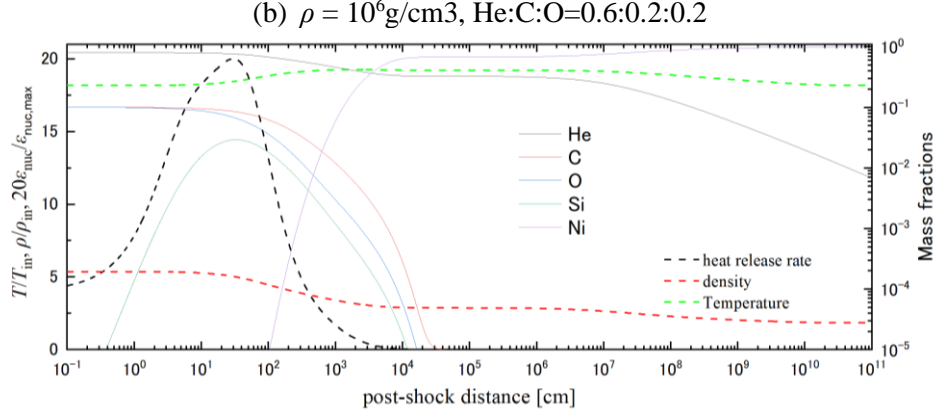
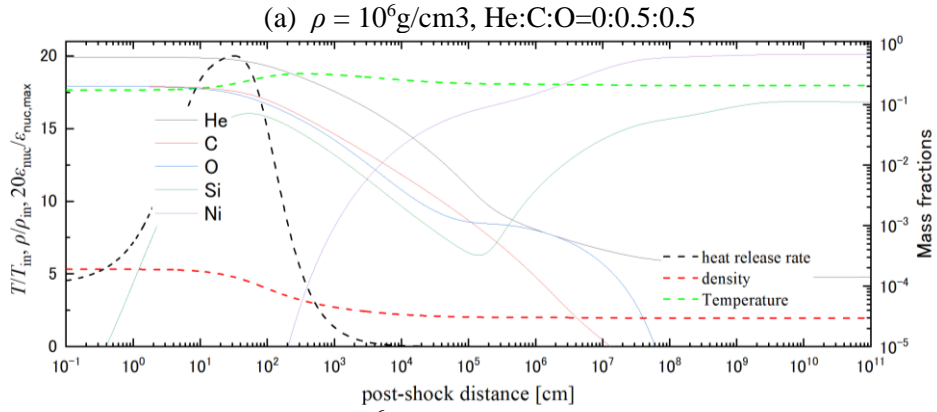
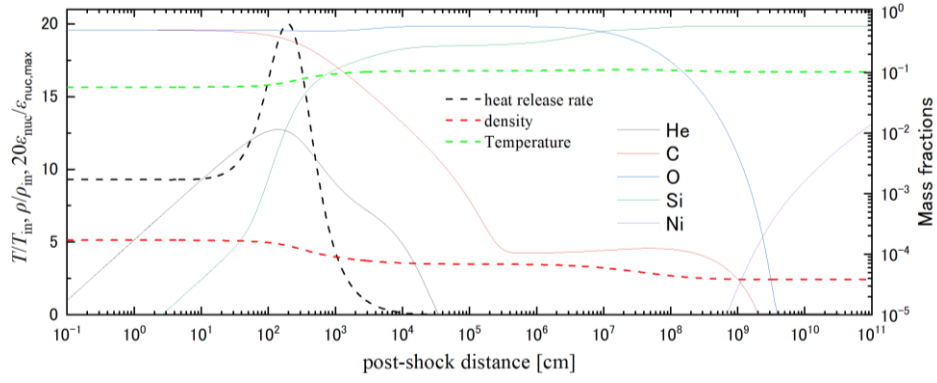


Figure 1: 1D ZND profiles of temperature, density, energy generation rate, and mass fractions of the isotopes.

Euler equations are solved including the transport equation of 13 isotopes (${}^4\text{He}$, ${}^{12}\text{C}$, ${}^{16}\text{O}$, ${}^{20}\text{Ne}$, ${}^{24}\text{Mg}$, ${}^{28}\text{Si}$, ${}^{32}\text{S}$, ${}^{36}\text{Ar}$, ${}^{40}\text{Ca}$, ${}^{44}\text{Ti}$, ${}^{48}\text{Cr}$, ${}^{52}\text{Fe}$, ${}^{56}\text{Ni}$). They are connected in an alpha chain, also including heavy-ion reactions (${}^{12}\text{C}+{}^{12}\text{C}$, ${}^{12}\text{C}+{}^{16}\text{O}$, and ${}^{16}\text{O}+{}^{16}\text{O}$) [3]. This thermonuclear reaction network is very stiff, as is so for the chemical reaction in detonation, for which an iterative implicit time integration of the Bader-Deuhrand scheme [8] is applied, while an explicit time integration of third-order TVD Runge-Kutta scheme is used to evolve the flow. AUSM+up scheme is used to discretize the convection term.

Density and composition are varied in the present study; temperature ahead of the shock front did not affect the post-shock structures. Therefore, $T = 2 \times 10^8$ K for every case. Density is varied $\rho = 10^5$ - 10^6 g/cm³, and helium mass fraction is varied between 0.0 – 0.8 with the rest being an equal amount of carbon and oxygen. This parameter space represents a reasonable range for the state of the ignition of the primary detonation in the WD envelope [11]. Helium mass fraction at the ignition spot depends on the mixing process induced by Kelvin-Helmholtz instability between the WD envelope and the accretion stream [12-14].



(a) $\rho = 10^6$ g/cm³, He:C:O=0:0.5:0.5, $\Delta = 20$ cm



(b) $\rho = 10^6$ g/cm³, He:C:O=0.6:0.2:0.2, $\Delta = 7$ cm



(c) $\rho = 10^6$ g/cm³, He:C:O=0.8:0.1:0.1, $\Delta = 7$ cm

Figure 2: Two-dimensional density contour of instantaneous detonation with variable helium mass fraction.

Results of ongoing two-dimensional simulations of detonation in the helium-rich matter are partly shown in Fig. 2 as the instantaneous density contour of each case. Except for the case with He:C:O=0.8:0.1:0.1 (Fig. 2(c)), strong transverse waves appeared, which forms multiple cellular structures throughout the domain: Around 9-12 cellular patterns are accommodated. When w/o helium case (Fig. 2(a)) and 60% helium case (Fig. 2(b)) are compared, w/o helium case exhibits a more irregular cellular motion: the peak density pattern and the spacing between the peaks is not constant for each cell. On the other hand, the cellular structure in the 60%-helium case is relatively regular. Also, the addition of helium reduces the cell width from $\sim 4 \times 10^3$ cm in the w/o helium case to $\sim 9 \times 10^2$ cm. This tendency is retained for the 70%-helium case, but in the 80%-helium case (Fig. 2(c)), the cellular pattern becomes too obscure to evaluate its cell width. This is the same for the smaller helium mass fraction, resulting in almost a planar detonation front without any significant instability. This occurred for other chosen grid resolutions, and may be attributed to a weaker sensitivity of the nuclear reaction to the strength of the shock front; the temperature behind the incident shock front is insensitive to the change of shock Mach number, because in the temperature range of 10^9 K radiation almost dominates internal energy, instead of thermal gas internal energy. However, the cellular structure of pure-helium detonation was similarly observed by Moore et al. [7], who numerically tested the effect of curvature on pure-helium detonation in the WD envelope. The detonations they simulated propagated at sub-C-J speed owing to the incompleteness of the reaction due to the limited reaction length in the actual WD length scale, and the velocity deficit induced by the curvature. This velocity-deficient detonation would be more sensitive to the disturbance of the shock, leading to instability emanating as transverse waves. This has been partly confirmed in our previous work, in which pure-helium detonation was observed to propagate around 70% of C-J velocity when the reaction is incomplete [15]. This issue should be addressed in more detail by simulating sub-C-J detonation in each case.

5 Future Prospects

C-J detonation is mainly discussed in the present study, which showed different behaviors of the thermonuclear reactions depending on helium mass fraction. As stated earlier, however, C-J detonation would not be likely to occur in the actual system in the WD envelope. Therefore, sub-C-J detonation in which the reaction is incomplete should be studied in our future works.

Acknowledgement

Our simulations were carried out on Cray XC50 at Center for Computational Astrophysics, National Astronomical Observatory of Japan and on Yukawa-21 at YITP in Kyoto University. This work was supported by JSPS KAKENHI Grant Number JP23K13146.

References

- [1] Gamezo, V. N., Wheeler, J. C., Khokhlov, A. M., Oran, E. S. (1999). Multilevel structure of cellular detonations in type Ia supernovae. *Astrophys. J.* 512: 827.
- [2] Timmes, F. X., Zingale, M., Olson, K. et al. (2000). On the cellular structure of carbon detonations. *Astrophys. J.* 543: 938.
- [3] Timmes, F. X., <https://cococubed.com>.
- [4] Nomoto, K. (1982). Accreting white dwarf models for type I supernovae. II. Off-center detonation supernovae. *Astrophys. J.* 257: 780.
- [5] Livne, E. (1990). Successive detonations in accreting white dwarfs as an alternative mechanism for Type I supernovae. *Astrophys. J.* 354: L53.

- [6] Jiang, J.-A., Doi, M., Maeda, K. et al. (2017). A hybrid type Ia supernova with an early flash triggered by helium-shell detonation. *Nature* 550: 80.
- [7] Moore, K., Townsley, D. M., Bildsten, L. (2018). The effects of curvature and expansion on helium detonations on white dwarf surfaces. *Astrophys. J.* 776: 97.
- [8] Bader, G., Deulhard, P. (1983). A Semi-Implicit Rule for Stiff Ordinary Differential Equations. *Numer. Math.* 41: 373.
- [9] Chapman, D. L. (1899). On the rate of explosion in gases. *Phil. Mag.* 47: 90.
- [10] Timmes, F. X., Niemeyer, J. C. (2000). Regimes of helium burning. *Astrophys. J.* 537: 993.
- [11] Iwata, K., Maeda, K. (2022). One-dimensional numerical study on ignition of the helium envelope in dynamical accretion during the double-degenerate merger. *Astrophys. J.* 941: 87.
- [12] Shen, K. J., Moore, K. (2014). The initiation and propagation of helium detonations in white dwarf envelopes. *Astrophys. J.* 797: 46.
- [13] Guillochon, J., Dan, M., Ramirez-Ruiz, E., Rosswog, S. (2010). Surface detonations in double degenerate binary systems triggered by accretion stream instabilities. *Astrophys. J.* 709: L64.
- [14] Tanikawa, A., Nomoto, K., Nakasato, N., Maeda, K. (2019). Double-detonation models for Type Ia supernovae: trigger of detonation in companion white dwarfs and signatures of companions' stripped-off materials. *Astrophys. J.* 885: 103.
- [15] Iwata, K., Maeda, K. (2022). Cellular structure of helium detonation as a trigger of sub-Chandrasekhar mass Type Ia supernovae, 28th Int. Colloq. Dyn. Explos. Reac. Sys., Napoli, Italy, June 19-24.